ELSEVIER

Journal of Photochemistry and Photobiology A: Chemistry 109 (1997) 47–52

Journal of PHOTOCHEMISTRY AND PHOTOBIOLOGY A:CHEMISTRY

Photochemical water oxidation to oxygen at the solid/gas interface of AgCl on zeolite A

Franz Saladin [a], Ivo Kamber [a], Klaus Pfanner [b], Gion Calzaferri [b,*]

[a] *Paul Scherrer Institute, 5232 Villigen PSI, Switzerland*

[b] *Department of Chemistry and Biochemistry, University of Bern, Freiestrasse 3, 3000 Bern 9, Switzerland*

Accepted 27 February 1997

Abstract

Silver chloride supported on zeolite A evolves oxygen when irradiated with light of wavelength shorter than about 550 nm in the presence of water-saturated argon. The amount of Ag^+ adsorbed on the surface of AgCl correlates with the photoreactivity of the system. The concentration of Ag^+ in the Ag^+/Na^+ zeolite A cages influences the rate at which oxygen is produced and determines the total amount formed. The reaction depends on the water partial pressure and the system shows self-sensitisation of the photochemical oxidation of water to oxygen, which means that new photoactive colour centres are formed under near UV illumination. A mechanism explaining the above findings is discussed. © 1997 Elsevier Science S.A.

Keywords: Photo-oxidation of water; Self sensitization; AgCl layers; Zeolite A; Oxygen evolution

1. Introduction

Photochemical water splitting remains one of the most challenging options for the photochemical conversion and storage of solar energy [1,2]. A widely used approach is to treat the water splitting reaction as two coupled half reactions. This facilitates the problem, as the anodic (oxidation of water) and the cathodic half reactions (reduction of protons) can be investigated separately. One would later try to combine the two reactions to form a complete water splitting system. The more difficult reaction of the two is the water oxidation because four electrons are involved in the formation of the final stable product O_2. It has been achieved with several systems containing AgCl [3,4]. On thin AgCl layers on supports like SnO_2-coated glass in contact with liquid water, quantum yields of 0.8 at 450 nm and 0.5 at 520 nm have been reported. The parameters controlling this reaction have been studied and a mechanism for the oxygen formation has been discussed which involves the formation of Cl_2 as an intermediate, followed by its reaction with water under formation of chloride and hypochlorous acid and the rapid Ag^+ catalysed disproportionation of the hypochlorous acid into chloride and molecular oxygen [4].

We were interested to know if and under what conditions the water oxidation could be observed upon irradiation of AgCl in contact with gaseous H_2O since no photochemical oxygen evolution from water with visible light at the solid/gas interface has been reported so far. A previously developed miniaturised photoreactor [5] coupled to a mass spectrometer proved to be a useful tool for the corresponding measurements. We have been able to measure significant photochemical oxidation of water to oxygen and by varying experimental conditions we have observed that the same mechanism that was invoked to explain the results obtained with AgCl in contact with liquid water holds for AgCl in contact with gaseous water. In contrast to the former system, however, Ag^+ containing zeolite support plays an important role in the latter due to its ion exchange capabilities.

2. Experimental

All chemicals used in the preparation of the samples and in the experiments were of analytical grade and only doubly distilled water (0.06 $\mu S\ cm^{-1}$) was used. Argon (99.998%) was used as carrier gas without further purification.

2.1. Sample preparation

Thin layers of silver chloride on a sapphire substrate were prepared by precipitation from equimolar amounts of silver nitrate and sodium chloride in the dark. After settling of the

* Corresponding author.

PII S1010-6030(97)00103-2

silver chloride, silver nitrate (5×10^{-3} M) was added to the solution above the layers. Ag^+ ions from the solution adsorb on the surface of the AgCl crystallites. One thus obtains silver chloride layers with a well defined concentration of silver ions at the surface. We call those [Ag^+/AgCl]. The layers were washed with water, dried at 70 °C and fixed with a drop of a PVC/THF solution (0.54 mg ml^{-1}).

Silver zeolite A (Ag^+-A zeolite) was prepared by ion exchange from commercial sodium zeolite (Na^+-A zeolite, Merck) with 0.1 M aqueous $AgNO_3$. Before further use the Ag^+-A zeolite was washed with water and dried at 70 °C. Layers of this material on sapphire were prepared by a technique described previously [6]: 20–40 mg Ag^+-A zeolite were suspended in 2 ml dioxane and sonicated for 5 min. 20 μl of this suspension were transferred onto the sapphire substrate and left to settle. Then the solvent was left to evaporate. The samples were dried at 70 °C and fixed with a drop of a PVC/THF solution (0.54 mg ml^{-1}). To ensure that only the centre of the substrate is covered, the outer part was screened by adhesive tape. The clean part of the sapphire substrate later acts as seal in the photoreactor. Layers prepared in this way contain 200–400 μg Ag^+-A zeolite and are approximately 1.5–3 μm thick. AgCl-covered Ag^+-A zeolite layers were prepared under red light from these samples. The so-prepared sapphire windows were mounted in a special Teflon tool [5] that covers the outer part of the window and forms a cylindrical receptacle above the Ag^+-A zeolite layer. A 0.1 M aqueous NaCl solution was transferred into the receptacle. While in contact with the NaCl solution, Ag^+ ions from inside the zeolite are exchanged for Na^+ ions and AgCl precipitates onto the outside surface of the zeolite microcrystals. The samples were then washed twice with H_2O.

Finally the Na^+/Ag^+ ratio within the zeolite microcrystals and the concentration of adsorbed Ag^+ on the AgCl precipitates were individually adjusted to the desired values by bringing the samples into contact with a solution containing adjusted amounts of Ag^+ and Na^+. The Ag^+/Na^+ ratio within the zeolite is determined solely by the Ag^+/Na^+ ratio in the surrounding solution [7] according to

$$\frac{[Ag^+]z}{[Na^+]z}\approx 500\frac{[Ag^+]_{aq}}{[Na^+]_{aq}} \quad (1)$$

while the amount of adsorbed Ag^+ is determined by the absolute Ag^+ concentration in the solution. Equilibrating the [AgCl]–Na^+-A zeolite samples with 10^{-3} M $AgNO_3$ solution leads to 100% Ag^+-exchanged zeolite, [Ag^+/AgCl]–$Ag^+{}_{12}$A. 50% and 9% Ag^+-exchanged zeolites, [Ag^+/AgCl]–$Ag^+{}_6$A and [Ag^+/AgCl]–$Ag^+{}_{1.1}$A, are obtained with $Na^+/Ag^+ = 500$ (0.5 M $NaNO_3/10^{-3}$ M $AgNO_3$) and $Na^+/Ag^+ = 5000$ (5 M $NaNO_3/10^{-3}$ M $AgNO_3$) respectively. In this series, the Ag^+ concentration in the solutions was kept constant, therefore the amount of Ag^+ adsorbed at AgCl is the same in all three samples.

[Ag^+/AgCl]–$Ag^+{}_6$A layers with different amounts of Ag^+ adsorbed on the surface of AgCl were prepared using

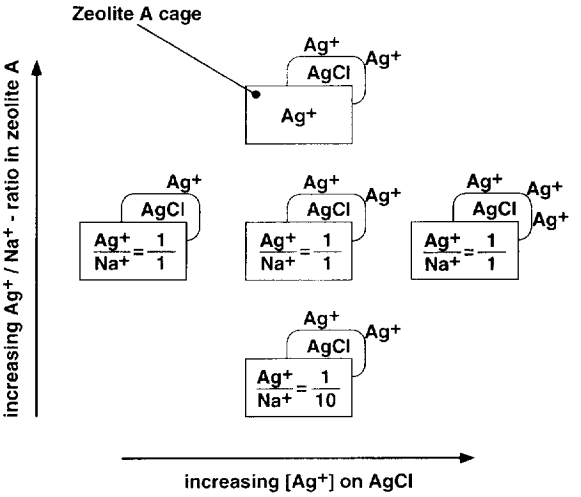

Scheme 1. Samples used to investigate the influence on the photochemical water oxidising ability of Ag^+/AgCl on $Ag^+{}_x Na^+{}_{12-x}$A zeolite. Horizontally: samples with different amount of Ag^+ adsorbed on AgCl. Vertically: samples with different Ag^+ exchange degrees (x) in the zeolite A.

solutions with the same Na^+/Ag^+ ratio but various Ag^+ concentrations. Using (2.5 M $NaNO_3/5\times10^{-3}$ M $AgNO_3$), (0.5 M $NaNO_3/10^{-3}$ M $AgNO_3$) and (0.1 M $NaNO_3/2\times10^{-4}$ M $AgNO_3$) yielded samples with decreasing Ag^+ concentrations on AgCl, respectively. The samples prepared in this way are illustrated in Scheme 1.

2.2. Photochemical experiments

The photochemical experiments were performed in a miniaturised photoreactor explained in detail in Ref. [5]. Two sapphire windows (∅ 12.7 mm, 2 mm thick) are fixed with flanges to both sides of a 0.5 mm thick metal ring thereby forming a small cylindrical compartment of 0.05 ml (ϕ 11 mm × 0.5 mm height). This volume is filled with gaseous reactants through 0.1 mm high and 1 mm wide channels inside the metal ring. The volume of the reactor, including these channels, totals to 0.06 ml. The sapphire windows are covered on the inner side with the photoactive solid that is irradiated through the window. If the samples are not fully absorbing, both windows are covered to increase the signal.

Detection of gaseous products was performed using a mass spectrometer (MS). The MS was calibrated by filling the reactor with known amounts of oxygen in argon and subsequently measuring the concentration with the MS while the reactor was purged. The detection limit for oxygen in the reactor was 100 ppm. In preliminary experiments none of the possible reaction products ClOH or Cl_2 could be detected. This can be explained as due to their high reactivity towards any surface in the set-up. Therefore experiments were focused on the detection of O_2 only, and no calibration for other species was performed.

A 200 W Hg/Xe lamp was used as the light source. IR radiation was blocked by a cooled water filter ($e = 10$ cm). A filter wheel, holding up to six filters, was placed in front of the light source. Filters used were 365 and 436 nm (LCP10-

X-R, Laser Components GmbH) and 540 nm (FS10-50, Andover Corporation). Light intensities were regulated by metallic neutral density filters and measured by a radiometer. To measure irradiances on-line, part of the light was reflected by means of a fused silica beam splitter onto a silicon photodiode. As the number of absorbed photons could not be determined, the number of photons impinging on the sample was used to calculate an apparent quantum yield. Since photons scattered off the sample are neglected, apparent quantum yields observed by that means mark the lower limit of the true quantum yields as they overestimate the number of absorbed photons.

The Ar carrier gas was passed through a water bubbler allowing to control the water partial pressure by keeping the bubbler at a certain temperature.

3. Results

AgCl supported on monograin layers of silver zeolite A exhibits appreciable water oxidation capabilities. Fig. 1 shows the in situ formation of O_2 at room temperature upon illumination of 2×300 μg [Ag^+/AgCl]–Ag^+_{12}A zeolite with near UV light.

A continuous flow of water-saturated argon (H_2O partial pressure 50 mbar) was passed through the reactor (1 ml min^{-1}) and to the MS, where the O_2 concentration in the gas was monitored. After 1 min in the dark, the sample was irradiated with 3.7 mW cm^{-2} at 365 nm. Under irradiation the O_2 formation set in and increased rapidly until it reached a maximum after about 1.5 min. It then decreased, more rapidly at first, and ceased as soon as the light was turned off after 31 min. In the same figure the integrated amount of evolved oxygen is also displayed. The smaller diagram shows an enlargement of the first three minutes of the experiment together with the on-line measured irradiance.

In contrast, neither Ag^+/AgCl layers nor pure Ag^+-A zeolite layers in contact with water-saturated argon showed water oxidation capabilities. Ag^+/AgCl was irradiated at room temperature at 365 nm. No oxygen was observed up to water partial pressures of 300 mbar and irradiances up to 4.1 mW cm^{-2}. In the case of pure Ag^+-A zeolite irradiated at 365 nm ($p(H_2O)=200$ mbar, $I=4.1$ mW cm^{-2}), no O_2 could be detected either.

The formation of oxygen at AgCl supported on monograin layers of silver zeolite A was found to depend strongly on the partial pressure of water in the argon feed. Fig. 2 shows the total amount of oxygen formed on 300 μg [Ag^+/AgCl]–Ag^+-A zeolite irradiated for 50 min at different water partial pressures ($I=4.1$ mW cm^{-2}, $\lambda=365$ nm). The oxygen evolution increases with increasing $p(H_2O)$ and reaches its maximum at $p(H_2O)=50$ mbar. This value corresponds to the practical limit for our experiment if no special precautions are taken to prevent condensation of water in the set-up.

Fig. 3 shows the influence of the Ag^+ exchange degree in the AgCl covered zeolite (Scheme 1) on the water oxidation

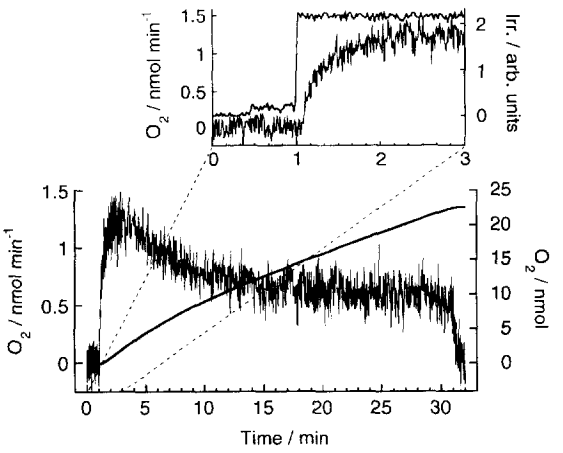

Fig. 1. In situ oxygen evolution rate (left scale, light line) and integrated amount of O_2 formed (right scale, heavy line) at 2×300 μg [Ag^+/AgCl]–Ag^+_{12}A. $\lambda=365$ nm, $I=3.7$ mW cm^{-2}, $p(H_2O)=50$ mbar. The inset shows the first 3 min of the experiment when the light was turned on. On the inset the signal monitoring the light source is also displayed (heavy line).

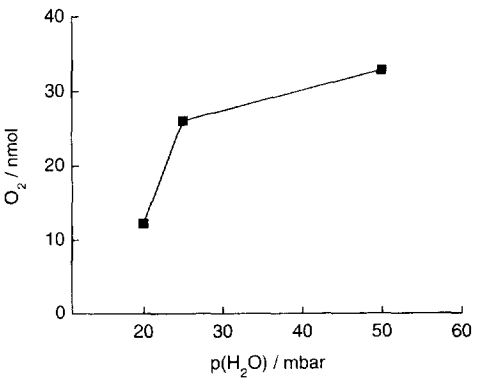

Fig. 2. Oxygen evolution at 300 μg [Ag^+/AgCl]–Ag^+_{12}A as function of the water partial pressure, $p(H_2O)$. In each experiment the sample was irradiated for 50 min. $I=4.1$ mW cm^{-2}, $\lambda=365$ nm.

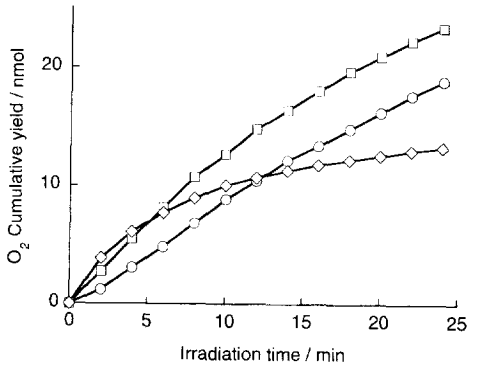

Fig. 3. Influence of the Ag^+ contents in the Ag^+/Na^+ zeolite A on the photo-oxidation of water. ○, [Ag^+/AgCl]–Ag^+_{12}A; □, [Ag^+/AgCl]–Ag^+_6A; ◇, [Ag^+/AgCl]–$Ag^+_{1.1}$A.

reaction. Layers consisting of 400 μg material with different Ag^+ exchange degrees, namely [Ag^+/AgCl]–Ag^+_{12}A, [Ag^+/AgCl]–Ag^+_6A and [Ag^+/AgCl]–$Ag^+_{1.1}$A were irradiated with 2.8 mW cm^{-2} at 313 nm ($p(H_2O)=50$ mbar). In these experiments products were accumulated within the photoreactor for 2 min. After every irradiation a dark experiment was performed to measure the oxygen background signal. The initial rate of oxygen formation as well as

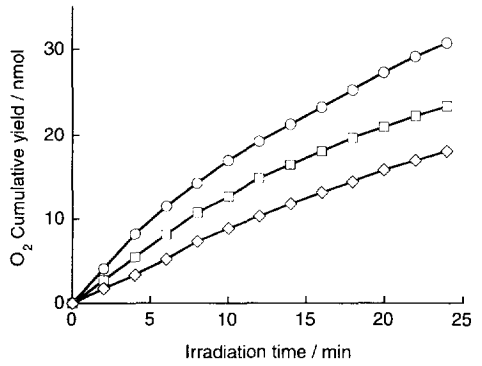

Fig. 4. Influence of the Ag^+ concentration on the surface of AgCl on the photo-oxidation of water. The Ag^+ concentration increases with increasing concentrations in the last step of the sample preparation. ◇, 2×10^{-4}M; □, 1×10^{-3}M; ○, 5×10^{-3}M.

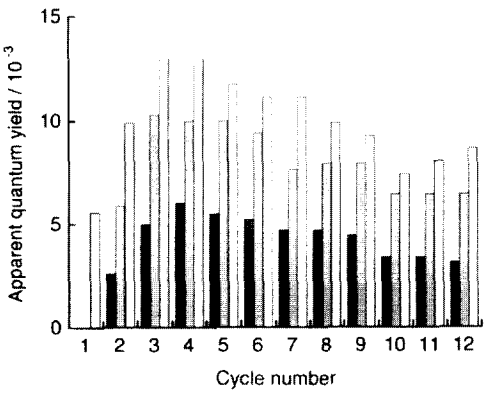

Fig. 5. Apparent quantum yields for the oxygen evolution at [Ag^+/AgCl]–$Ag^+{}_6$A irradiated at: □, 365 nm; □, 436 nm (×4); and ■, 540 nm (×20): calculated from (moles $O_2\times4$) per mole photons impinging on the sample. In the first cycle, no oxygen is formed under green and blue light and only little under UV light. Through the UV irradiation, the sample becomes light sensitive also in the visible part of the spectrum and the apparent quantum yields increase for all wavelengths.

the final amount of oxygen formed strongly depends on the amount of Ag^+ within the zeolite. [Ag^+/AgCl]–$Ag^+{}_{1.1}$A initially shows the fastest oxygen evolution rate, but the reaction slows down rapidly. In contrast to this behaviour oxygen is formed on [Ag^+/AgCl]–$Ag^+{}_{12}$A with the slowest initial rate but the rate does only marginally decrease within the 25 min of illumination shown in Fig. 3. The behaviour of [Ag^+/AgCl]–$Ag^+{}_6$A lies in between the two former cases. Over a longer period of time (not shown in the graph) the total O_2 yield was found to be highest for [Ag^+/AgCl]–$Ag^+{}_{12}$A, lowest for [Ag^+/AgCl]–$Ag^+{}_{1.1}$A and for [Ag^+/AgCl]–$Ag^+{}_6$A it was laying in between the two extremes.

Experiments to investigate the effect of different amounts of the Ag^+ ions adsorbed at AgCl (Scheme 1) were conducted under the same conditions as above. In Fig. 4, cumulative yields of oxygen for 400 μg samples of [Ag^+/AgCl]–$Ag^+{}_6$A are shown. The samples differ in the Ag^+ concentration of the solution used in the last step of the sample preparation. The respective concentrations were 5×10^{-3} M, 1×10^{-3} M and 2×10^{-4} M. The photoactivity of the samples correlates well with the amount of silver ions on their surface. The fastest oxygen formation is observed for the samples with the largest amount of Ag^+ adsorbed on AgCl.

Self-sensitisation in the water oxidation reaction at [Ag^+/AgCl]–$Ag^+{}_6$A could be observed as illustrated by the measured apparent quantum yields in Fig. 5. To maximise the oxygen signal, thus increasing the sensitivity, both windows of the photoreactor were covered with [Ag^+/AgCl]–$Ag^+{}_6$A in this experiment. The front window facing the light source was covered with 300 μg material while the back window was covered with 400 μg. The experiment was performed at $p(H_2O) = 70$ mbar and products were accumulated for 220 sec inside the photoreactor. The sample was irradiated at three different wavelengths, starting with green light (540 nm, 6.4 mW cm^{-2}), then blue light (436 nm, 1.6 mW cm^{-2}) and finally UV light (365 nm, 0.2 mW cm^{-2}). Between the irradiations the sample was kept in the dark for 220 s to accumulate the background signal. This cycle, dark–540 nm–dark–436 nm–dark–365 nm, was repeated 12 times. The results are shown in Fig. 5. In the first cycle, no oxygen was formed under green and blue light and only little under UV light. Starting with the second cycle, [Ag^+/AgCl]–$Ag^+{}_6$A becomes light sensitive also in the visible part of the spectrum and the apparent quantum yields increase for all wavelengths. After 44 min total irradiation time the apparent quantum yields slowly decrease.

4. Discussion

We have observed significant photochemical oxidation of water to oxygen at the solid/gas interface. In these experiments, liquid water was only present in minute quantities of a thin film of physisorbed water that covers the surface of the samples. The thickness of the film depends to a certain degree on the water partial pressure in the surrounding atmosphere. This is an important difference to previously reported experiments which were performed at solid/liquid water interfaces [3,4].

In the water oxidation reaction protons are released, according to

$$2H_2O \rightarrow O_2 + 4H^+ + 4e^- \quad (2)$$

If the photochemical oxygen formation described in the experimental part is due to this redox reaction, we expect an immediate and drastic pH drop at the very beginning of the irradiation because the produced protons remain confined in the small volume of the film as illustrated in Fig. 6. In earlier investigations we have found that the optimum pH for the photo-oxidation of water is around pH 4–6 depending on the conditions. In more acidic environment no oxygen is evolved, and the same is true for a pH higher than 9 [4]. The inhibition of oxygen evolution at low pH can explain the fact that no oxygen was found in the case of pure AgCl. Other products may have been formed, but it was not possible to detect them with the described apparatus.

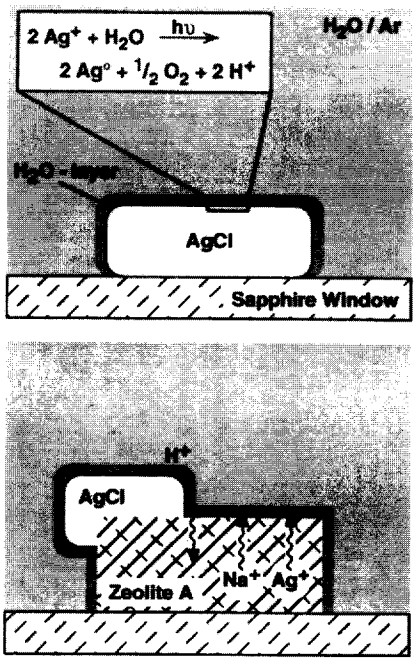

Fig. 6. Mechanism of the photochemical water oxidation at Ag^+/AgCl. Top: pure Ag^+/AgCl. Bottom: Ag^+/AgCl supported on $Ag^+_xNa^+_{12-x}A$ zeolite.

AgCl was proven to be the photoactive part in our experiments by using pure silver zeolite, not containing any AgCl. No oxygen was found in this case. The zeolite part however plays an important role. One of its most important features are the ion exchange properties. Zeolite A shows a high selectivity for cations like Ag^+ [7–9] and these cations can be exchanged for protons. In the experiments with AgCl on zeolite A we took advantage of these properties. The zeolite acts as a pH buffer where protons are exchanged for sodium or silver ions. When silver chloride on zeolite A is illuminated under the above described conditions, oxygen is evolved because the pH drop is much less pronounced due to the buffer effect of the zeolite. Sodium zeolite is better suited for this purpose than silver zeolite because Na^+ ions are more readily exchanged by protons than Ag^+ ions. This is illustrated in Fig. 3. Samples with less Ag^+ in the zeolite show a higher initial oxygen evolution rate than samples with high Ag^+ exchange degree. The water film on the surface of the samples is necessary for an ion exchange between the surface of the AgCl and the zeolite. A larger amount of liquid water on the sample helps to damp the pH drop induced by the photoreaction. Therefore the reaction works the better, the higher the water partial pressure is in the surrounding atmosphere. This can be deduced from the results illustrated in Fig. 2.

The oxygen evolution rate depends on the Ag^+ concentration applied in the last step of the sample preparation. Larger Ag^+ concentrations result in a higher photochemical activity of the samples. The adsorption of Ag^+ in a solution contacting silver chloride is well known [10]. The larger the concentration in the solution the more Ag^+ is adsorbed on the surface of the silver chloride. The most photoactive sample therefore contains the largest amount of silver ions on its surface. This seems to parallel observations made in silver halide photography studies [10,11].

It has been reported that the number of interstitial silver ions [12,13] as well as the negative surface charge increase with increasing Cl^- concentration. At high chloride concentration and low pH the photoproduct is chlorine [14]. In our set-up a huge surface (capillaries, MS) is exposed to the products. Reactive products such as Cl_2 or ClOH readily chemisorb on these surfaces. This prevents us from detecting them as intermediates or as final photoproducts.

The total amount of O_2 formed depends on a second effect also related to the ion exchange properties of the zeolite. The silver ions on the surface of the silver chloride are reduced during the illumination and after some time the surface situation becomes less favourable for oxygen evolution. Since the surface, however, is in ion exchange equilibrium with the ions in the zeolite, part of the photochemically reduced silver ions on the silver chloride are replaced by silver ions ofthe zeolite. Therefore the final amount of oxygen formed depends on the total amount of Ag^+ in the system. The less Na^+ within the zeolite was exchanged by Ag^+ the smaller is the amount of oxygen produced. This is illustrated in Fig. 3 where after 25 min hardly any oxygen is evolved for [Ag^+/AgCl]–$Ag^+_{1.1}A$ while for [Ag^+/AgCl]–Ag^+_6A and [Ag^+/AgCl]–$Ag^+_{12}A$ oxygen formation is sustained. The sample with the highest silver exchange degree shows a small initial oxygen evolution rate but the slowest drop in photoactivity. The results shown in Fig. 5 demonstrate that the self-sensitisation effect, which was found and described at the solid/liquid interface [4,15,16] is also present under the entirely different conditions described in this work. We assume that the underlying mechanism is the same, meaning that new colour centres are formed due to the accumulation of reduced silver clusters that form during the reaction.

5. Conclusions

We have found that silver chloride on zeolite A is able to oxidise water forming oxygen when irradiated with near UV light in the presence of water-saturated argon. The reaction shows the same type of self-sensitisation as reported for silver zeolite suspensions and thin silver chloride layers in contact with the liquid phase. In this process, the formation of new colour centres shifts the absorptivity well into the visible region (see also Refs. [3,4,14–17]). The apparent quantum yield that was found in the corresponding experiments is calculated from the number of photons impinging on the sample and therefore marks the lower limit of the true quantum yield. In addition these values should be considered with care since surface concentrations that strongly influence the systems capacity cannot be easily controlled in these experiments. The zeolite, being in ion exchange equilibrium with the thin water film covering the samples, acts as a buffer for

photoformed protons, exchanging them with sodium or silver ions from the zeolite cages. The pH is thus kept in a range favouring the oxygen evolution. We do not know its actual value, however. The silver ions exchanged for the protons do take part in the photoreaction. The photoactivity of the samples is influenced by the amount of silver ions adsorbed on the surface of the silver chloride. The total amount of oxygen produced is controlled by the total amount of Ag^+ present at the AgCl surface and in the zeolite which acts as a reservoir.

During the water oxidation with silver chloride, Ag^+ is reduced. In order to make the process useful for solar energy conversion, these silver species must be reoxidised to form a reversible system. Recent photoelectrochemical experiments conducted with Ag^+/AgCl layers on conducting SnO_2 and other electrodes at the solid/liquid water interface gave encouraging results in that simultaneous photochemical oxygen evolution and anodic oxidation of the reduced silver could be observed over many hours [18].

Acknowledgements

This work has been supported by the Swiss Federal Office of Energy, grant numbers 55022 and BEW-EPA 217.307.

References

[1] R.J. Marcus, Science 123 (1956) 399.
[2] A.J. Bard, M.A. Fox, Acc. Chem. Res. 28 (1995) 141.
[3] G. Calzaferri, N. Gfeller, K. Pfanner, J. Photochem. Photobiol. A: Chem. 87 (1995) 81.
[4] K. Pfanner, N. Gfeller, G. Calzaferri, J. Photochem. Photobiol. A: Chem. 95 (1996) 175.
[5] F. Saladin, A. Meier, I. Kamber, Rev. Sci. Instrum. 67 (1996) 2406.
[6] R. Beer, F. Binder, G. Calzaferri, J. Photochem. Photobiol. A: Chem. 69 (1992) 67.
[7] J. Li, K. Pfanner, G. Calzaferri, J. Phys. Chem. 99 (1995) 2119.
[8] H.S. Sherry, H.F. Walton, J. Phys. Chem. 71 (1967) 1457.
[9] D.W. Breck, Zeolite Molecular Sieves, J.W. Sons, New York, 1974.
[10] T.H. James, The Theory of the Photographic Process, Macmillan, New York, 4th edn., 1977.
[11] A.P. Marchetti, R.S. Eachus, in: D.H. Volman, G.S. Hammond, D.C. Neckers (eds.), Advances in Photochemistry, Wiley-Interscience, New York, 1992, Vol. 17, p. 145.
[12] H.A. Hoyen, Phenomena at Silver Halide Interfaces Requiring Additional Fundamental Understanding, in: A. Baldereschi (ed.), The Physics of Latent Image Formation in Silver Halides, Trieste, Italy, 1983.
[13] Y.T. Tan, J. Chem. Soc. Faraday Trans. 2 85 (1989) 457.
[14] (a) G. Calzaferri, W. Spahni, Chimia 40 (1986) 435. (b) G. Calzaferri, W. Spahni, J. Photochem. 32 (1986) 151.
[15] B. Sulzberger, G. Calzaferri, J. Photochem. 19 (1982) 321.
[16] G. Calzaferri, S. Hug, T. Hugentobler, B. Sulzberger, J. Photochem. 26 (1984) 109.
[17] G. Calzaferri, Catal. Today, in press.
[18] M. Lanz, G. Calzaferri, J. Photochem. Photobiol. A: Chem. 109 (1997) 87–89.